

Quantitative Assessment of Phase Change Material Utilization for Building Cooling Load Abatement in Composite Climatic Condition

Rajat Saxena

Centre for Energy Studies,
Indian Institute of Technology, Delhi,
Hauz Khas, Delhi 110016, India

Kumar Biplab

GreenTree Building Energy Pvt. Ltd.,
Noida 201301, India

Dibakar Rakshit¹

Centre for Energy Studies,
Indian Institute of Technology, Delhi,
Hauz Khas, Delhi 110016, India
e-mail: dibakar@iitd.ac.in

The global trend of energy consumption shows that buildings consume around 48% of the total energy, of which, over 50% is for heating and cooling applications. This study elucidates on cooling load reduction with phase change material (PCM) incorporation in a building envelope. PCM provides thermal shielding due to isothermal heat storage during phase change. PCM selection depends upon its phase change temperature, thermal capacity, and thermal conductivity, as they play a vital role in assessing their impact on energy conservation in buildings. The uniqueness of this study underlies in the fact that it focuses on the utilization of PCM for New Delhi (28.54°N , 77.19°E) climatic conditions and adjudges the suitability of three commercially available PCMs, based on the overall heat load reduction and their characteristic charging/discharging. The study aims at finding an optimum melting and solidification temperature of the PCM such that it may be discharged during the night by releasing the heat gained during the day and mark its suitability. The results of mathematical modeling indicate that as per the design conditions, the melting/solidification temperature of 34°C is suitable for New Delhi to absorb the peak intensity of solar irradiation during summer. Based on the thermophysical properties in literature (Pluss Advanced Technologies Pvt. Ltd., 2015, "Technical Data Sheet of savE® HS29, PLUSS-TDS-DOC-304 Version R0," Pluss Advanced Technologies Pvt. Ltd., Gurgaon, India. Pluss Advanced Technologies Pvt. Ltd., 2015, "Technical Data Sheet of savE® OM32, PLUSS-TDS-DOC-394 Version R0," Pluss Advanced Technologies Pvt. Ltd., Gurgaon, India. Pluss Advanced Technologies Pvt. Ltd., 2012, "Technical Data Sheet - savEVR HS34, Doc:305," Pluss Advanced Technologies Pvt. Ltd., Gurgaon, India), mathematical modeling showed HS34 to be suitable for New Delhi among the three PCMs. To ratify this, characteristic charging and discharging of HS34 is tested experimentally, using differential scanning calorimeter (DSC). The results showed that HS34 is a heterogeneous mixture of hydrated salts having super-cooling of 6°C , reducing its peak solidification temperature to 30.52°C during the cooling cycle also making it unsuitable for peak summers in New Delhi. [DOI: 10.1115/1.4038047]

Keywords: latent heat storage, PCM panels, building energy conservation, characteristic charging/discharging, DSC

1 Introduction

We are living in a world where energy utilization per capita defines economy and living standards of people within a country. In tropical countries, major power consumption in summers is due to air-conditioning, causing greenhouse gas emissions. With an intent of reducing the power consumption, there is a need for systematic study to make buildings more energy efficient, without compromising the comfort level [1]. Keeping in view the thermal comfort requirements in places with extremes of temperatures, i.e., temperatures as high as 45°C in summers and as low as 6°C in winters, houses must be designed in such a way that the temperature variation inside the building envelope is within the acceptable limits and without hefty heating/cooling loads. Therefore, designing energy efficient houses demands utilization of materials, which result in increasing the thermal mass of roof/walls and limit the inside room temperature without increasing the actual construction size. Phase change material (PCM) incorporation

within the building envelope can be a lucrative option for building heat load abatement with minimal active cooling load requirements. The benefit of using PCM is that it stores large amount of energy (latent heat) at a particular temperature/range, i.e., the phase change temperature, thereby increasing the overall energy density of the building wall.

Cabeza et al. [2], Hauer et al. [3], Khundhair and Farid [4], and Zalba et al. [5] have discussed different PCMs, their thermal performance and their incorporation in gypsum boards. Jeong et al. [6] have carried out thermal performance evaluation studies of shape stabilized Bio-PCMs. Pokhrel et al. [7] have discussed the impact on the thermal properties of PCM composites of medium temperature (melting point 80°C) and graphite. The composite PCM thermal energy storage is numerically analyzed and optimized for maximum efficiency of the thermal energy storage. The study also deals in thermal characterization of the candidate PCMs. Kaushik et al. [8] have given the thermal modeling of a space, neglecting the periodic variation in the ambient air temperature, solar influx and wind speed, thus, suitable for comparison of different structures but not for determining the actual temperature within a building. Pashupathy et al. [9] have shown the mathematical modeling and simulation comparison for climatic conditions of Chennai, with PCM incorporated roof. Kosny et al.

¹Corresponding author.

Contributed by the Solar Energy Division of ASME for publication in the JOURNAL OF SOLAR ENERGY ENGINEERING. Manuscript received March 27, 2017; final manuscript received September 23, 2017; published online October 17, 2017. Assoc. Editor: Jorge Gonzalez.

Table 1 Criteria for climatic zones in India [18]

Type	Climate	Relative humidity (%)	Mean monthly temperature (°C)
I	Hot and dry	<55	>30
II	Warm and humid	>55	>30
III	Moderate	<75	25–30
IV	Cold and cloudy	>55	>25
V	Cold and sunny	<55	>25
VI	Composite	This applies when six months or more do not fall within any of the above categories	

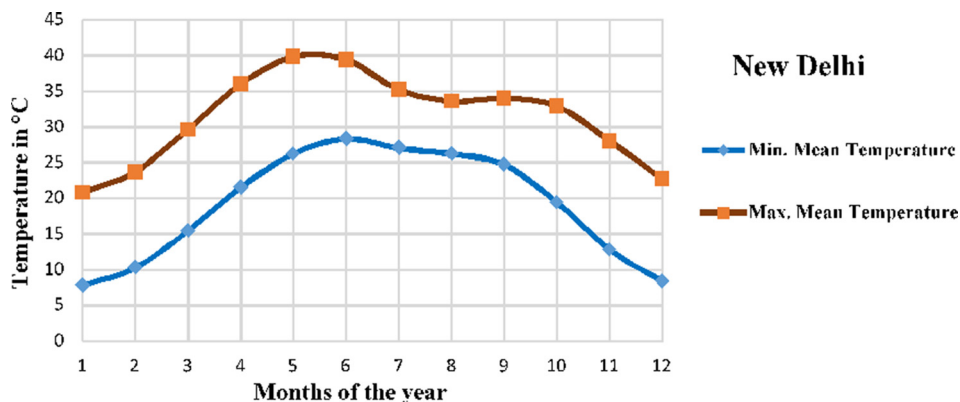
[10] have discussed the application of PCM as a heat sink over the roof, achieving about 50% cooling and 30% heating load reductions in East Tennessee, USA. Rahman et al. [11] and Krishnan et al. [12] have performed modeling of solid–liquid phase change problem for PCMs. Sleiti and Naimester [13,14] have reported enhanced stabilizing effect on the inner surface temperature with a PCM enhanced ceiling; however, there was an insignificant change in zone mean air temperature for U.S. based commercial restaurant building. Entrop et al. [15] have assessed the implementation of PCMs for residential buildings in The Netherlands. Mavrigiannaki and Ampatzis [16] have discussed different latent heat storage in building elements using PCM to contribute in reducing loads and achieving energy savings with careful designing of the PCM elements. Ascione et al. [17] have discussed the energy refurbishment of existing buildings through the use of PCM and assessed its impact in terms of energy savings and indoor comfort for the cooling season in Mediterranean region. All these studies enumerate the benefits of PCM utilization in buildings; however, they do not mention the criteria to adjudge the suitability of a PCM for a particular location/climatic condition.

The present work describes thermal modeling of a room with PCM embedded walls/roof and demonstrates the suitability of commercially available PCMs for New Delhi. This study is divided into two parts, the first dealing with a detailed mathematical modeling of a PCM embedded room, while the second part

dealing with the assessment of PCMs, based on their characteristic charging and discharging. Salient features of this study are that the building model takes into account the variation in solar influx, wind velocity, and ambient temperature on hourly basis, which are otherwise approximated and cannot be parameterized to gauge PCM impact. It focusses on finding a suitable phase change temperature of the PCM that can be associated with New Delhi so that a commercial PCM product for heat load reduction can be introduced.

2 Design Conditions and Geometry

2.1 Design Conditions. The weather and climatic conditions of a particular place are characterized by the solar irradiation, ambient temperature, humidity, precipitation, sky conditions, and wind velocity. Further, the solar irradiation depends on latitude, longitude, time of the day, time of the year, orientation, etc. The climatic zones are categorized based on the annual climatic variations. India has six climatic zones. Table 1 gives the criteria for division of these climatic zones. This study is carried out for New Delhi, which falls under composite climatic zone. The mean average temperature of New Delhi during winters is around 8 °C and around 40 °C during summers, as shown in Fig. 1. This results in large temperature variation within the building space. To

**Fig. 1 Average monthly minimum and maximum temperature for New Delhi****Table 2 Thermal properties and application of the selected PCMs [19–21]**

PCMs	Base material	Thickness (mm)	Thermal conductivity (W/mK) (solid)	Thermal conductivity (W/mK) (liq.)	Melting temperature (°C)	C_p (kJ/kg K) (solid)	C_p (kJ/kg K) (liq.)	Latent heat (kJ/kg)	Density (solid) kg/m ³ at 291 K	Density (liq.) kg/m ³ at 313 K	Applications
HS29	Inorganic salt mixture	25	0.478	0.382	29	1.9	2.3	190	1830	1530	Currently apart from building application, used for biopharmaceutical transportation, milk product/food/poultry storage systems and for telecommunication as heat sink applications.
HS34	Inorganic salt mixture	25	0.5	0.47	34	1.9	2.35	150	1980	1850	
OM32	Organic mixture	25	0.219	0.145	32	1.95	2.3	200	928	870	

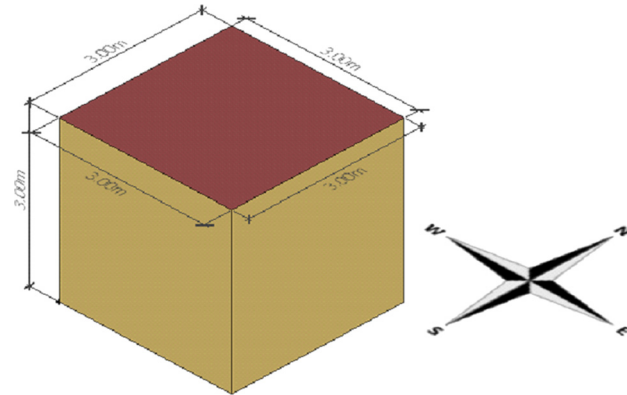


Fig. 2 Test room specifications

minimize this temperature variation, the thermal mass of the building walls/roofs must be increased, which is possible with PCM integration within the walls/roof.

A mathematical modeling is carried out for first week of May as it has highest mean peak temperature during the year. The average maximum temperature during first week of May is well above 35°C , and average minimum temperature is around 27°C . For a PCM to work efficiently, it must regenerate during off-sunshine hours, which requires a sufficient temperature difference

between the phase change and ambient air temperature. For this study, three PCMs having phase change temperatures of 29°C (HS29) [19], 32°C (OM32) [20], and 34°C (HS34) [21] are chosen, as their phase change temperatures lie within the minimum and maximum temperatures of Delhi for summers. Table 2 shows the thermo-physical properties and application of these PCMs. The PCM thickness is an important parameter, which controls the amount of PCM that is applied. However, it should not be very large or else PCM may not discharge completely, thereby reducing its utility. This is because during discharging, the solid PCM layer formed inhibits the heat transfer process. The thicker it gets, the heat flow from the liquid PCM toward the lower temperature region decreases, thus, reducing the discharge rate of the PCM.

2.2 Geometry. A test room is designed, as shown in Fig. 2, with dimensions $3\text{ m} \times 3\text{ m} \times 3\text{ m}$ and walls made up of brick (thickness 110 mm), with a layer of plaster (gypsum thickness 15 mm) on each side. PCM is placed within a 1 mm thick tedler enclosure, on the outside, as shown in Fig. 3(a). The thickness of the PCM layer is 15 mm. Therefore, the total thickness of the composite wall is 157 mm. Thus, the PCM thickness is kept relatively smaller compared to the wall thickness. It is observed that for present configuration increasing the thickness beyond this would affect the heat transfer as discussed in the previous sub-heading. The roof is made of concrete (thickness 200 mm) and plastered on both sides and PCM applied, as shown in Fig. 3(b).

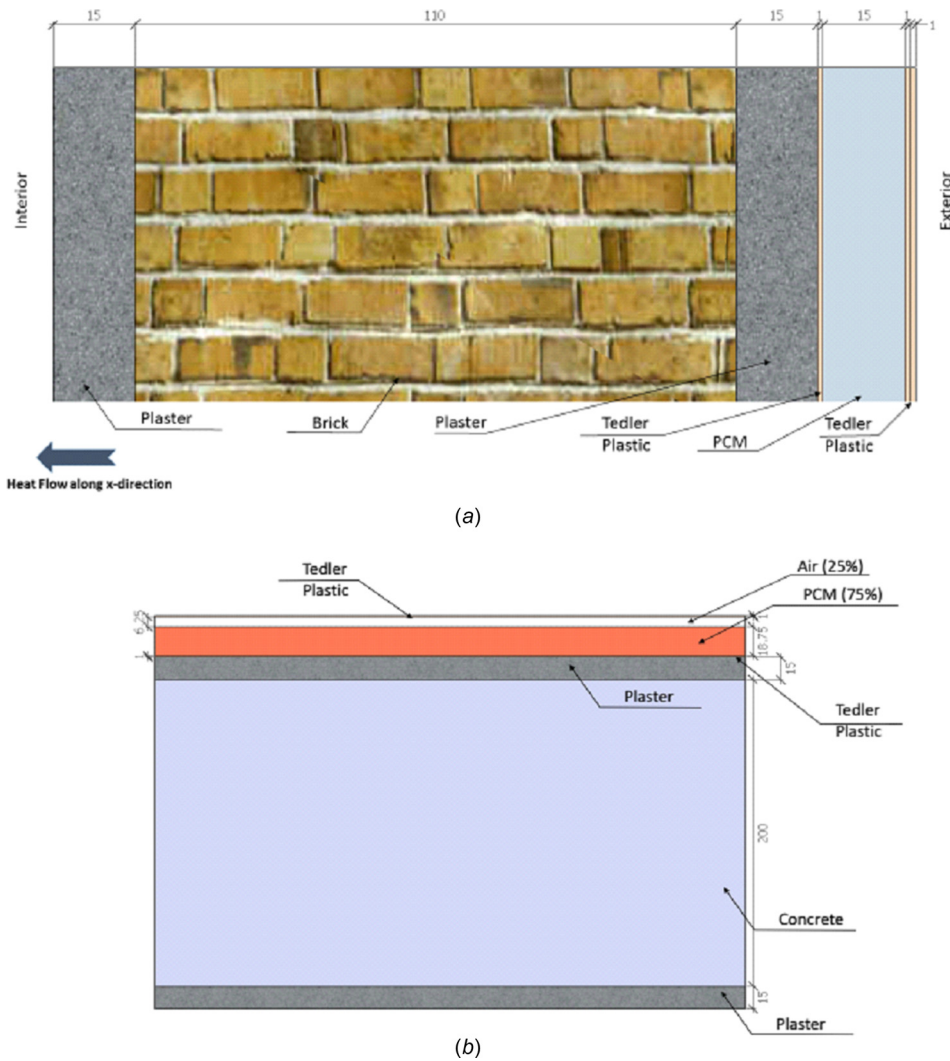


Fig. 3 (a) and (b) Schematic diagram of wall cross section and roof cross section with PCM

Incident Solar Radiation falling on different surfaces

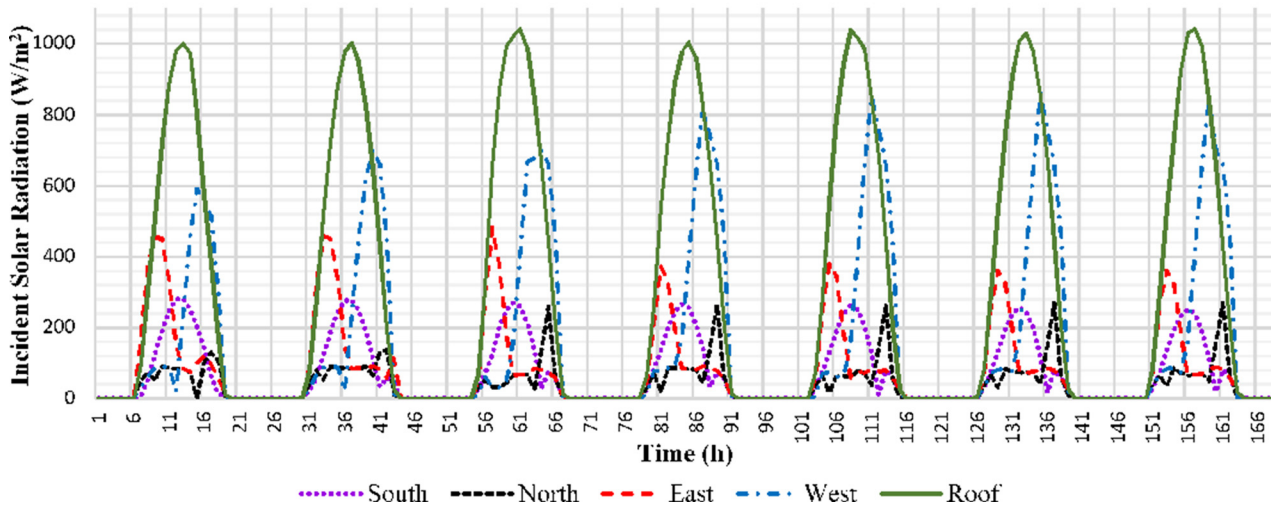


Fig. 4 Incident solar radiation on different surfaces

3 Mathematical Formulation and Methodology

Following are the mathematical assumptions:

- I. One dimensional heat transfer, along x-direction (Fig. 3(a)), is considered.
- II. Constant room temperature (25°C).
- III. Uniform PCM temperature (equal to the mean temperature of the interface across the PCM layer).
- IV. For HS29, the density difference at 18°C (solid) and 40°C (liquid) is found to be maximum (Table 1). The percentage change in density with respect to liquid PCM is around 19.6%. Therefore, keeping the factor of safety in conception, an empty space of 25% by volume is assumed for the expansion of PCM.

To estimate the PCM impact, the first thing is to find the ambient temperature and incident solar radiation. In this study, incident direct and diffused components of the incoming solar radiation data and the wind speed are taken from ISHRAE [22]. The incident solar radiation is different for different walls/roof and is required for determining the solar air temperature [23], given by

$$T_{\text{sol}} = T_a + \left(\frac{\alpha I - \varepsilon \Delta R}{h_o} \right) \quad (1)$$

where " T_a " is the ambient temperature, " α " is absorptivity of the material, and ε is the emissivity of the surface.

ΔR = Rate of exchange of long wavelength radiation between air and sky.

$\varepsilon \Delta R \approx 60 \text{ W/m}^2$ (For Roof) (For vertical wall, this term is 0)
 h_o is calculated using Mc Adams equation [22]:

$$h_o = 5.7 + 3.8 V \quad \text{for } 0 < V < \frac{5m}{s} \quad (2)$$

where "V" is the ambient wind velocity.

The solar-air temperature depends on the following factors:

- tilt of the surface (with the horizontal " β "),
- orientation of the tilted surface (surface azimuth angle " γ "),
- location (latitude " φ "),
- time of the day (hour angle " ω "),
- day of the year (declination angle " δ ").

The following relation gives the value of " I " falling on the different surfaces of the room:

$$I = I_b \left(\frac{\cos \theta_t}{\cos \theta_z} \right) + I_d \left(\frac{1 + \cos \beta}{2} \right) + \rho_{\text{ground}} (I_b + I_d) \left(\frac{1 - \cos \beta}{2} \right) \quad (3)$$

where ρ_{ground} represents the reflected component from the ground. " I " reaching the surface is calculated taking into account only the beam and diffused components of the solar radiation.

Values of " $\cos \theta_t$ " and " $\cos \theta_z$ " are calculated from the following relations [23]:

$$\begin{aligned} \cos \theta_t &= (\cos \phi \cdot \cos \beta + \sin \phi \cdot \sin \beta \cdot \cos \gamma) \cos \delta \cdot \cos \omega \\ &\quad + \cos \delta \cdot \sin \omega \cdot \sin \beta \cdot \sin \gamma \\ &\quad + \sin \delta (\sin \phi \cdot \cos \beta - \cos \phi \cdot \sin \beta \cdot \cos \gamma) \end{aligned} \quad (4)$$

$$\cos \theta_z = (\cos \phi \cdot \cos \delta \cdot \cos \omega + \sin \delta \cdot \sin \phi) \quad (5)$$

Surface azimuth angle " γ " is 0° , -180° , -90° , and 90° for south, north, east, and west walls, respectively. Declination angle is calculated using the following relation [23]:

$$\delta = 23.45 \sin \left[\frac{360}{365} (284 + n) \right] \quad (6)$$

where "n" is the day of the year. The value of declination angle changes on daily basis. The hour angle symbolizes the time of the day and is calculated using following relation [23]:

$$\omega = (ST - 12) \times 15 \text{ deg} \quad (7)$$

where "ST" is the solar time. The relation between solar time and standard watch time is given as follows:

$$\text{solar time} - \text{standard time} = \pm 4(L_{\text{st}} - L_{\text{loc}}) + E \quad (8)$$

where L_{st} for India is $81^{\circ}54'$ and L_{loc} is the longitude of Delhi. "E" is the equation of time, which is given by

$$\begin{aligned} E &= 229.2(0.000075 + 0.001868 \cos B - 0.032077 \sin B \\ &\quad - 0.014615 \cos 2B - 0.04089 \sin 2B) \end{aligned} \quad (9)$$

where $B = (n - 1)360/365$ and "n" is the day of the year [23].

The values of " I ," i.e., the incident solar radiation on different walls and the roof of the room, are shown in Fig. 4. It shows the variation of " I " on hourly basis from May 1st to May 7th. The solar air temperature is calculated for hourly temperature variations between 7 am to 7 pm. Beyond these intervals, the temperature is kept equal to the ambient temperature. This variation of temperature along the day is as shown in Fig. 5.

Equation (10) is obtained through the principle of conservation of energy on a control volume (test room). Equations (11) and (12)

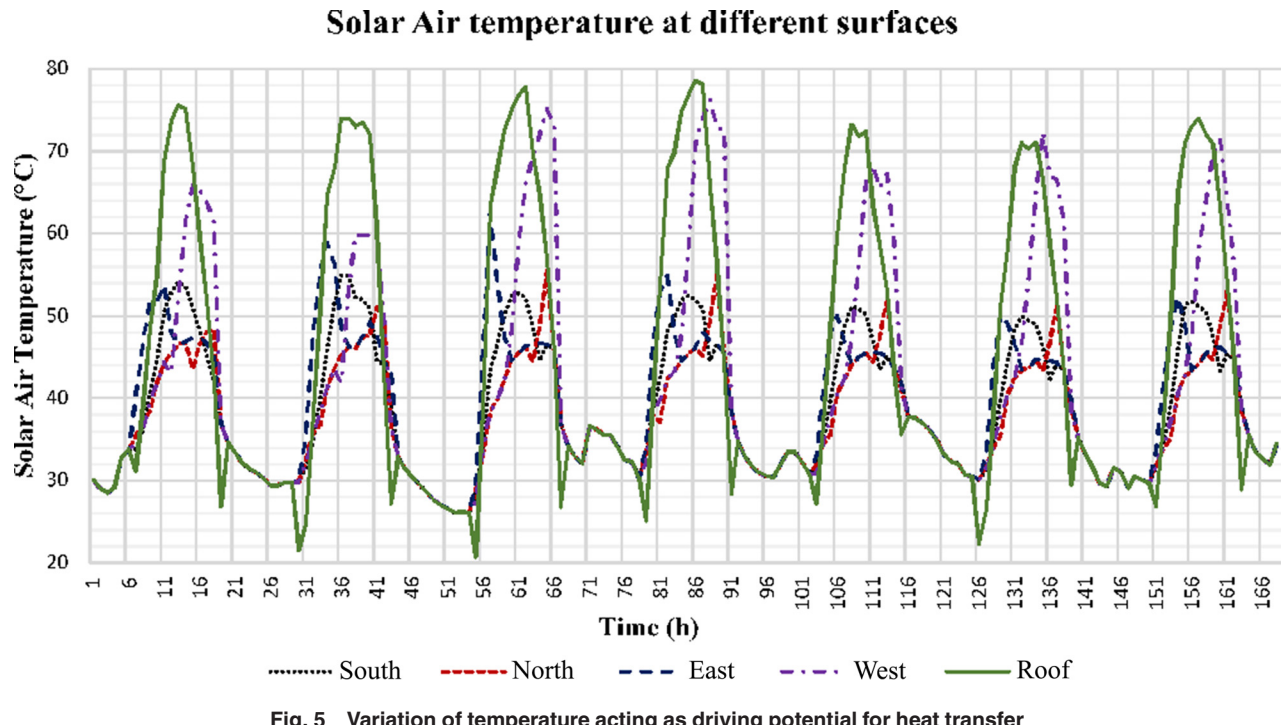


Fig. 5 Variation of temperature acting as driving potential for heat transfer

Table 3 Thermal resistances (R) and thermal capacitances (C) of the equivalent electrical network model [24]

Interface	1	2...n - 1	n
R	$\frac{1}{h_0 A_{\text{wall}}}$	$\frac{\Delta x_j}{k A_{\text{wall}}}$	$\frac{1}{h_i A_{\text{wall}}}$
C	$\rho_{\text{wall}} A_{\text{wall}} c_{p,1} \Delta x_1$	$\rho_{\text{wall}} A_{\text{wall}} c_{p,j} \Delta x_j$	$M_{\text{air}} c_{p,\text{air}}$

show the boundary conditions applied for the indoor and the ambient

$$\frac{dt_{\text{wall}}}{d\tau} = \alpha \frac{d^2 t_{\text{wall}}}{dx^2} \quad (10)$$

Boundary conditions:

For indoor:

$$-k \frac{dt_{\text{wall}}}{dx} \Big|_{x=0} = h_i(t_{\text{wall,in}} - t_i) \quad (11)$$

For ambient:

$$-k \frac{dt_{\text{wall}}}{dx} \Big|_{x=\delta'} = h_o(t_{\text{sol}} - t_{\text{wall,out}}) \quad (12)$$

Equation (12) shows the initial condition:

$$\tau = 0, \quad t_{\text{wall}}(x) = t_{\text{wall},0}, \quad \text{for } 0 \leq x \leq \delta' \quad (13)$$

$$Q_{hf,1} = \frac{t_{\text{sol}} - t_1}{R_1} \quad (15)$$

The heat flow ($Q_{hf,j}$) and heat stored ($Q_{st,j}$) within the wall material at any interface "j" are given by

$$Q_{hf,j} = \frac{t_{j-1} - t_j}{R_j}, \quad j = 1 \dots n \quad (16)$$

$$Q_{st,j} = C_j \frac{dt_j}{d\tau}, \quad j = 1 \dots n \quad (17)$$

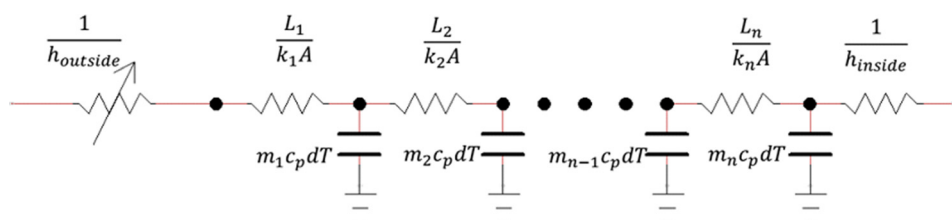
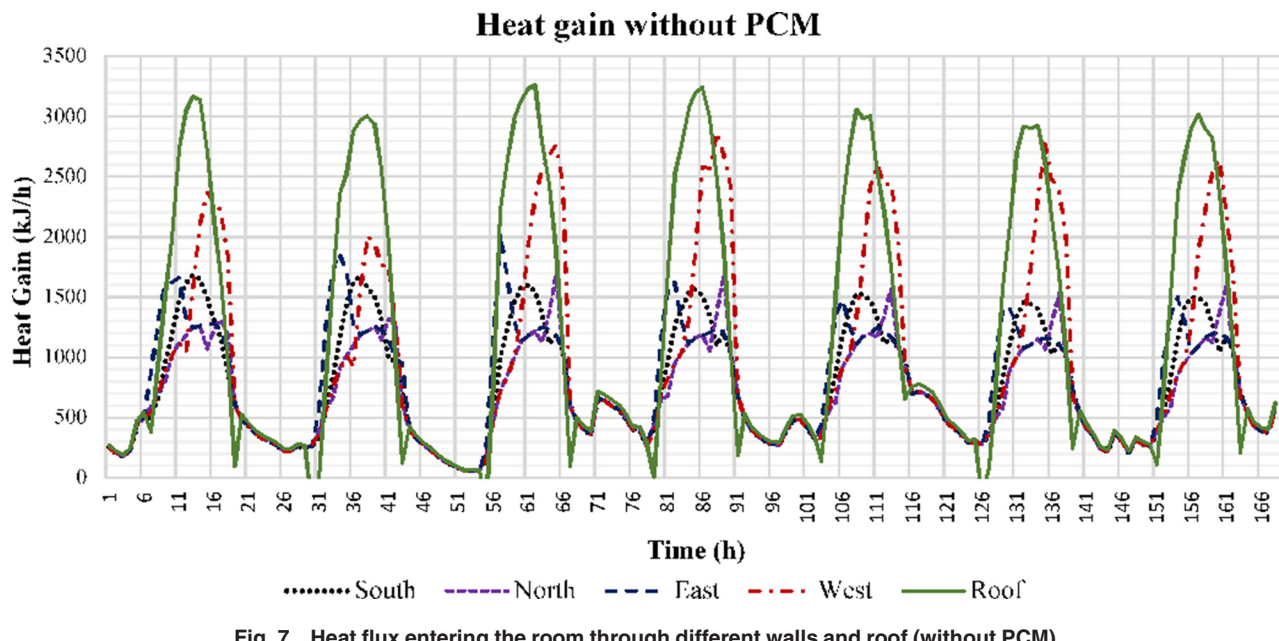


Fig. 6 Electrical circuit of a composite wall



All the calculations are done first without the application of PCM, and then by incorporating the selected PCMs one by one. Figure 7 shows the heat transfer to the conditioned space without PCM incorporation. For PCM incorporated walls/roof, the temperature at all the interfaces is determined on the basis of energy conservation. As already mentioned, the thickness of PCM is small; thus, its temperature is assumed equal to the mean temperature of the interface across the PCM layer. The PCM state is tracked based on this mean interfacial temperature. If this temperature is above or below the threshold phase change temperature, it undergoes sensible heating/cooling. However, if the temperature is equal to the phase change temperature, then heat flow results in the increase or decrease of heat stored within the PCM as latent heat comes into play. The temperature of PCM only increases once the

heat stored within it exceeds the overall latent heat capacity, which is equal to the product of latent heat and corresponding mass of the PCMs.

4 Validation

The analytical results obtained from the present model are validated against the experimental results of Pasupathy et al. For the same geometry, PCM temperature and ambient conditions, given in study [9], the inside wall temperature is calculated using present analytical model. The weather data for New Delhi is taken from ISHRAE [22]. Figure 8 shows the comparison between the analytical results, obtained using equations given in Sec. 3, and experimental results of Pasupathy et al. The theoretical results

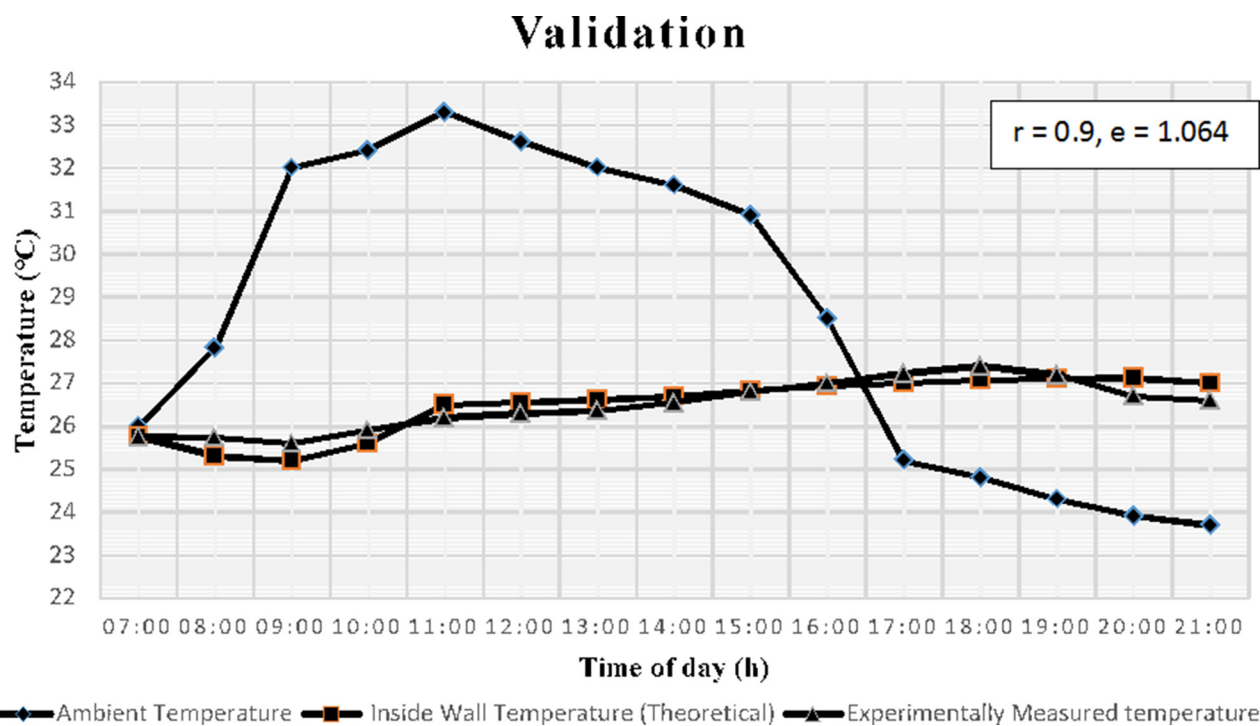


Table 4 Comparison between energy plus and analytical calculations

Date	HS 29					OM 32					HS 34				
	Local time	Energy plus	Analytical method	Percentage absolute difference	Mean absolute deviation	Local time	Energy plus	Analytical method	Percentage absolute difference	Mean absolute deviation	Local time	Energy plus	Analytical method	Percentage absolute difference	Mean absolute deviation
1-May	2:00	1452.09	1416.23	2.53	4.88	16:00	2689.15	2478.40	8.50	4.71	21:00	3073.30	3186.51	3.55	5.97
2-May	2:00	1288.22		9.04		16:00	2334.05		5.82		21:00	3331.03		4.54	
3-May	2:00	1395.47		1.47		16:00	2412.83		2.65		21:00	3006.54		5.65	
4-May	2:00	1378.51		2.66		16:00	2586.17		4.35		21:00	2891.06		9.27	
5-May	2:00	1292.79		8.72		16:00	2422.72		2.25		21:00	2968.79		6.83	

obtained through mathematical modeling show close conformance to the experimental results. To compare the two results, the correlation coefficient (r) and root mean square percentage deviation (e) are evaluated using the following relations [26]:

$$\text{correlation coefficient } r = \frac{N \sum X_i Y_i - (\sum X_i)(\sum Y_i)}{\sqrt{N \sum X_i^2 - (\sum X_i)^2} \sqrt{N \sum Y_i^2 - (\sum Y_i)^2}} \quad (18)$$

$r > 0$ implies positive linear relationship, $r < 0$ implies negative linear relationship, and $r = 0$ means no linear relationship between two variables.

$$\text{root-mean-square percentage deviation } e = \sqrt{\frac{\sum (e_i)^2}{N}} \quad (19)$$

where $e_i = [(X_i - Y_i)/X_i] \times 100$.

This shows the percentage deviation of experimental values of parameters (Y_i) from the theoretical values of parameters obtained from the mathematical modeling (X_i).

The results for heat gain are validated using ENERGYPLUS. A single thermal zone building, modeled in ENERGYPLUS, using finite difference algorithm is developed. The finite difference approach discretizes the walls, floors, and roofs into several nodes and uses

an implicit finite difference scheme to solve the heat transfer equations numerically. Equation (20) shows the calculation method used for the fully implicit scheme for a homogeneous material with uniform node spacing [27]

$$C_p \rho \Delta x \frac{T_i^{j+1}}{\Delta t} = k_w \frac{(T_{i+1}^{j+1} - T_i^{j+1})}{\Delta x} + k_E \frac{(T_{i-1}^{j+1} - T_i^{j+1})}{\Delta x} \quad (20)$$

where

$$k_w = \frac{(k_{i+1}^{j+1} - k_i^{j+1})}{2}$$

$$k_E = \frac{(k_{i-1}^{j+1} - k_i^{j+1})}{2}$$

$$k_i = k(T_i^{j+1})$$

T is the temperature, i is the node being modeled, $i-1$ is the adjacent node to the exterior of construction, $j+1$ is the new time-step, j is the previous time-step, Δt is the time-step, and Δx is the finite difference layer thickness.

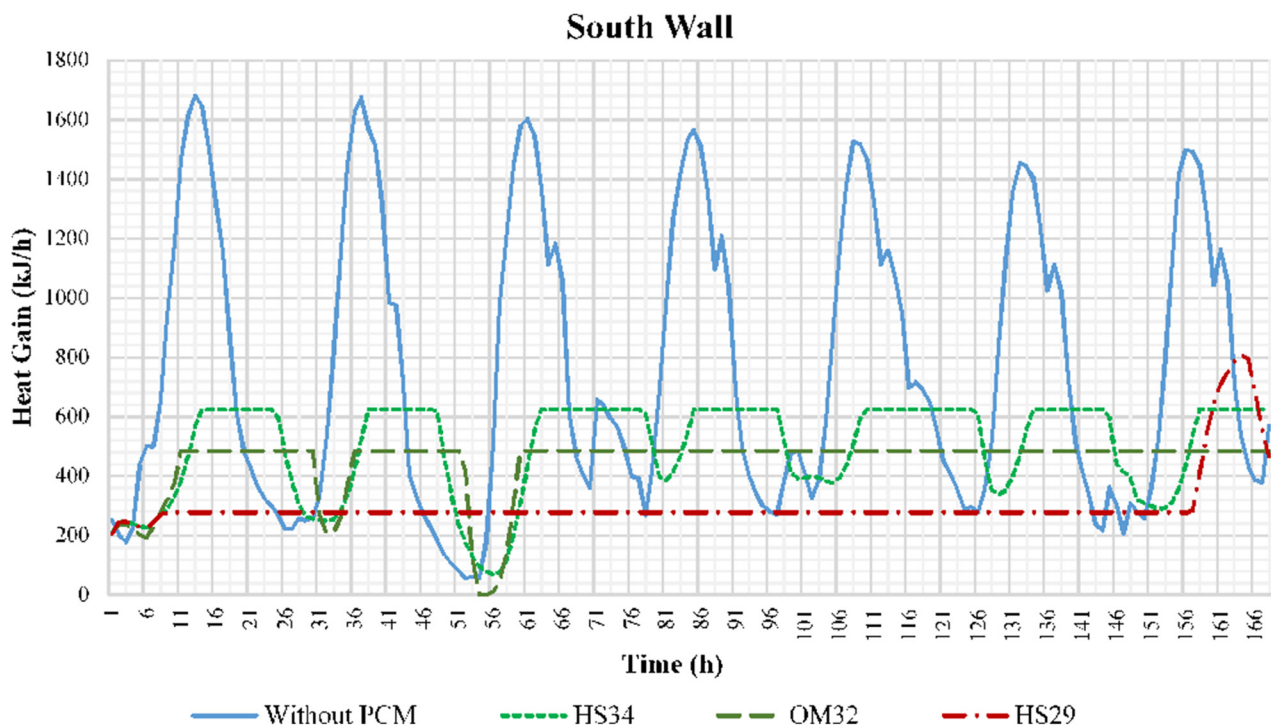


Fig. 9 Heat flux entering through south wall with and without PCMs

West Wall

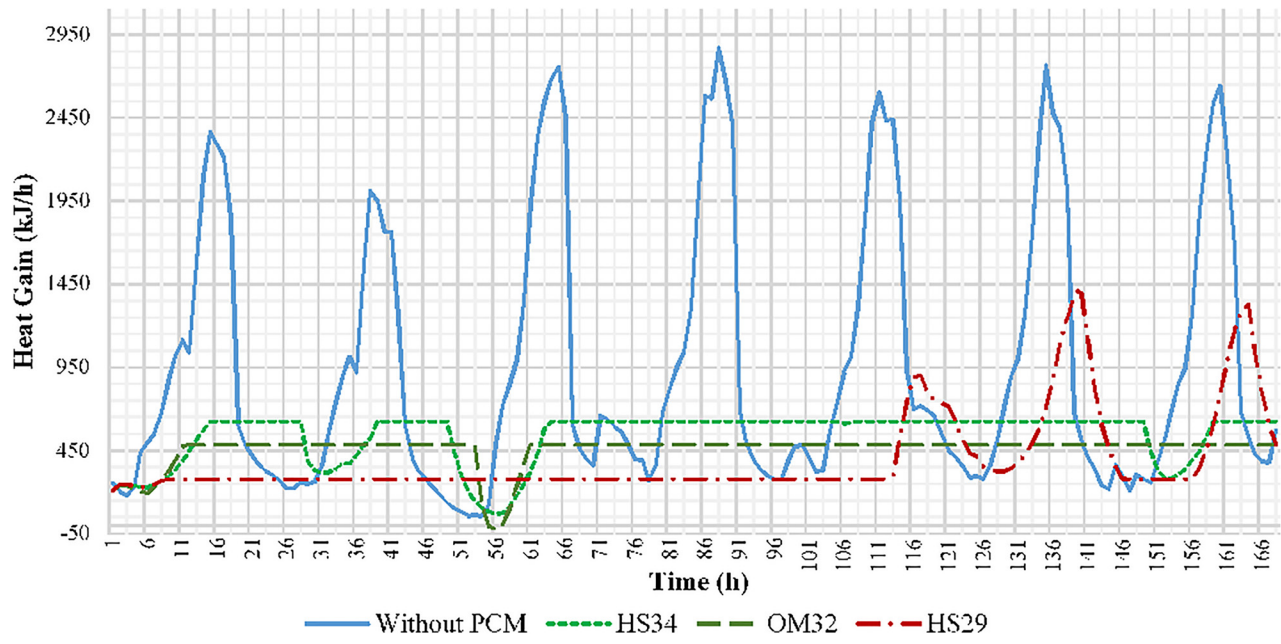


Fig. 10 Heat flux entering through west wall with and without PCMs

North Wall

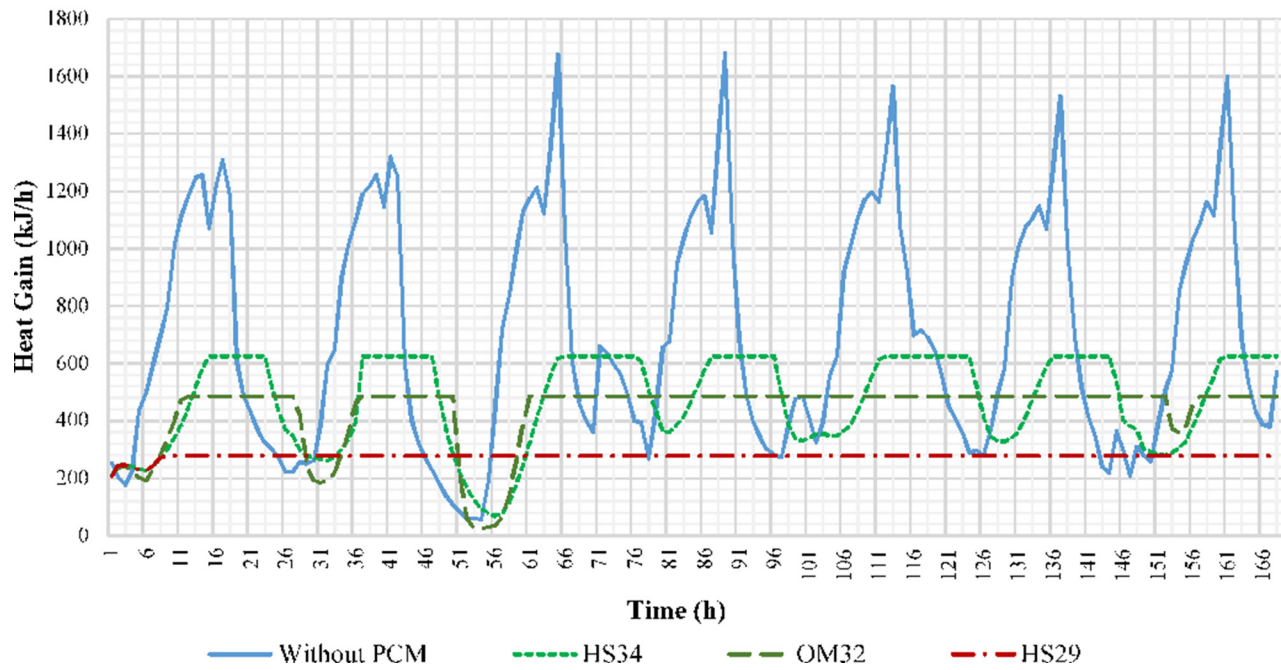


Fig. 11 Heat flux entering through east wall with and without PCMs

In the algorithm, all elements are divided or discretized automatically using Eq. (23), which depends on a space discretization constant (c), the thermal diffusivity of the material (α), and the time-step. Users can leave the default space discretization value of 3 (equivalent to a Fourier number (F_o) of 1/3) or input other values [26]

$$\Delta x = \sqrt{c \cdot \alpha \cdot \Delta t} = \sqrt{\frac{\alpha \cdot \Delta t}{F_o}} \quad (21)$$

"For the PCM algorithm, the method is coupled with an enthalpy-temperature function (Eq. (20)) that the user inputs to account

for enthalpy changes during the phase change [28]. To develop an equivalent specific heat at each time-step, an enthalpy-temperature function is used. The resulting model is a modified version of the enthalpy method" [28]

$$h = h(T) \quad (22)$$

$$c_p^*(T) = \frac{(h_i^j - h_i^{j-1})}{(T_i^j - T_i^{j-1})} \quad (23)$$

where h is the enthalpy.

East Wall

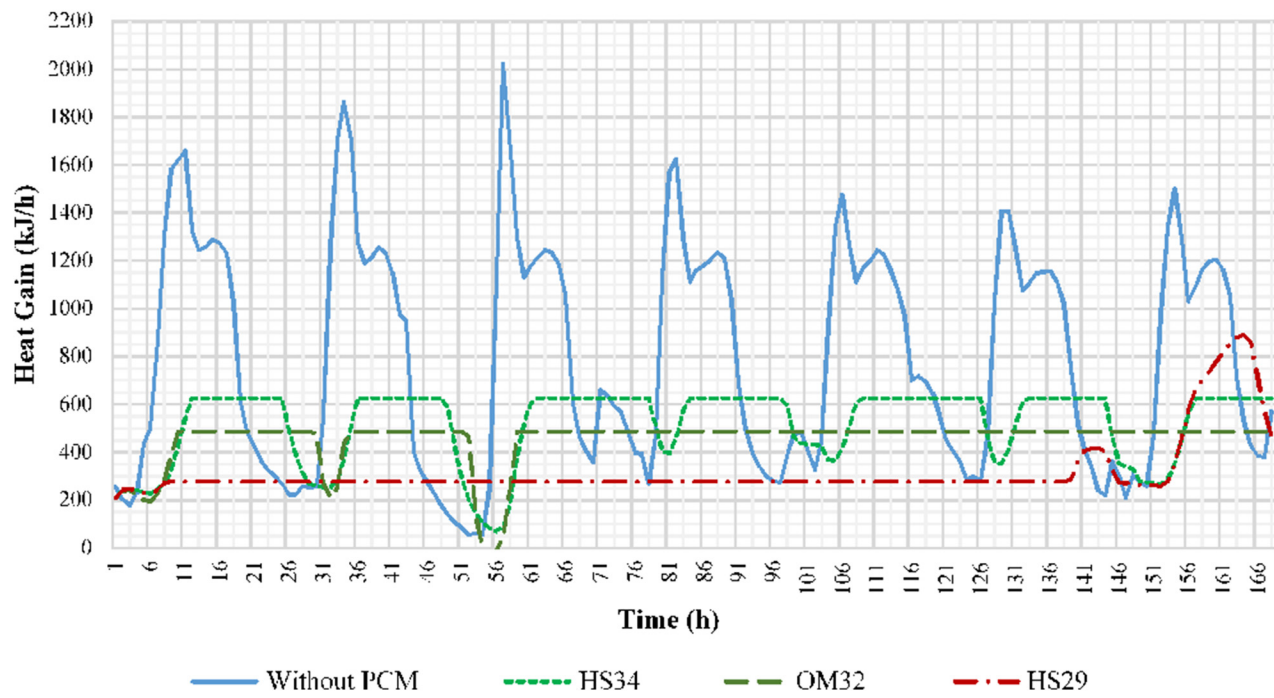


Fig. 12 Heat flux entering through north wall with and without PCMs

The construction build-up is similar to that as mentioned before. The indoor temperature of 25 °C is maintained by providing unlimited cooling. The infiltration rate for the room is set to zero air changes per hour. The internal gains are set to zero, in line with the calculations carried out above. Table 4 shows the comparison of the heat flux entering the conditioned space/control volume obtained analytically, as well as through ENERGYPLUS software for the first five days of May, at different times for all the

three PCMs. The mean absolute deviation in all the three cases is 4.88 for HS29, 4.71 for OM32, and 5.97 for HS34.

5 Results and Discussion

5.1 Comparison Between HS29, OM32, and HS34. Figure 9 compares the different heat flow profile for south wall for all the

Roof

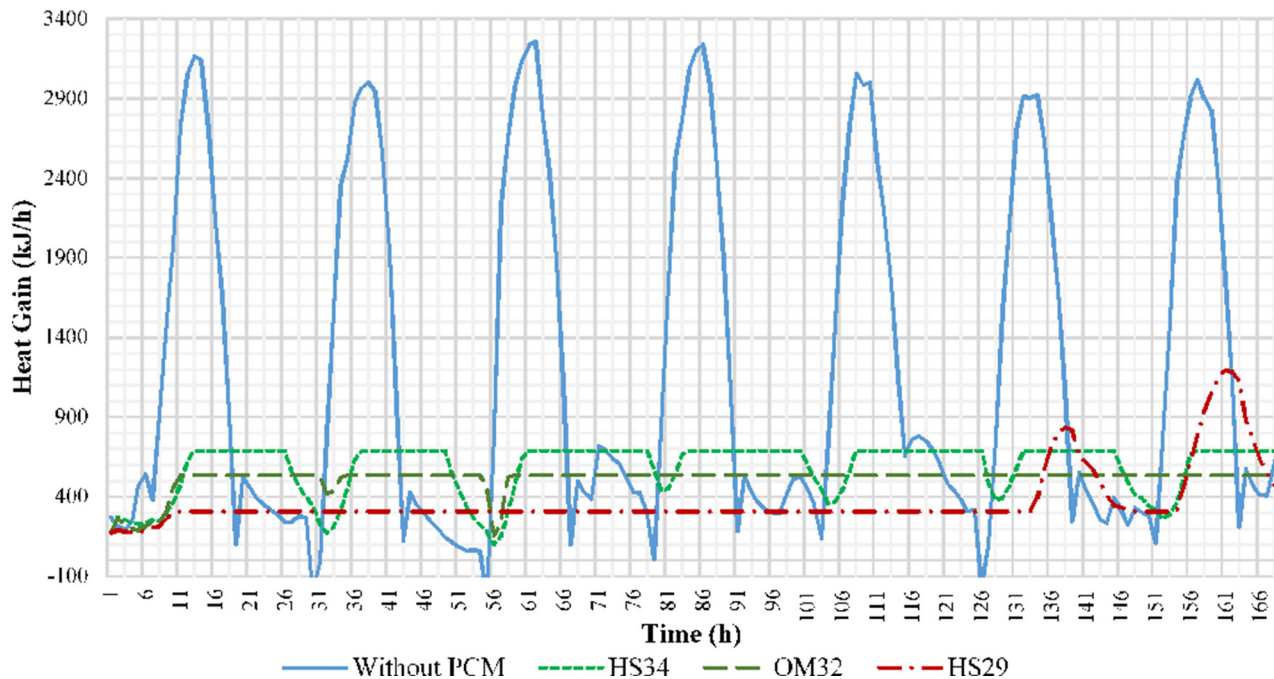


Fig. 13 Heat flux entering through roof wall with and without PCMs

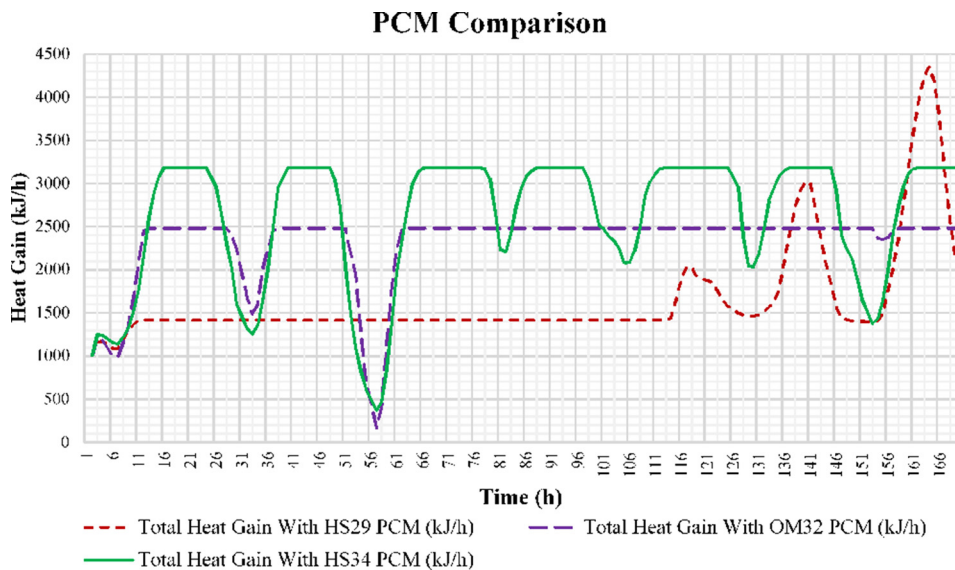


Fig. 14 Comparative heat gain with different PCMs

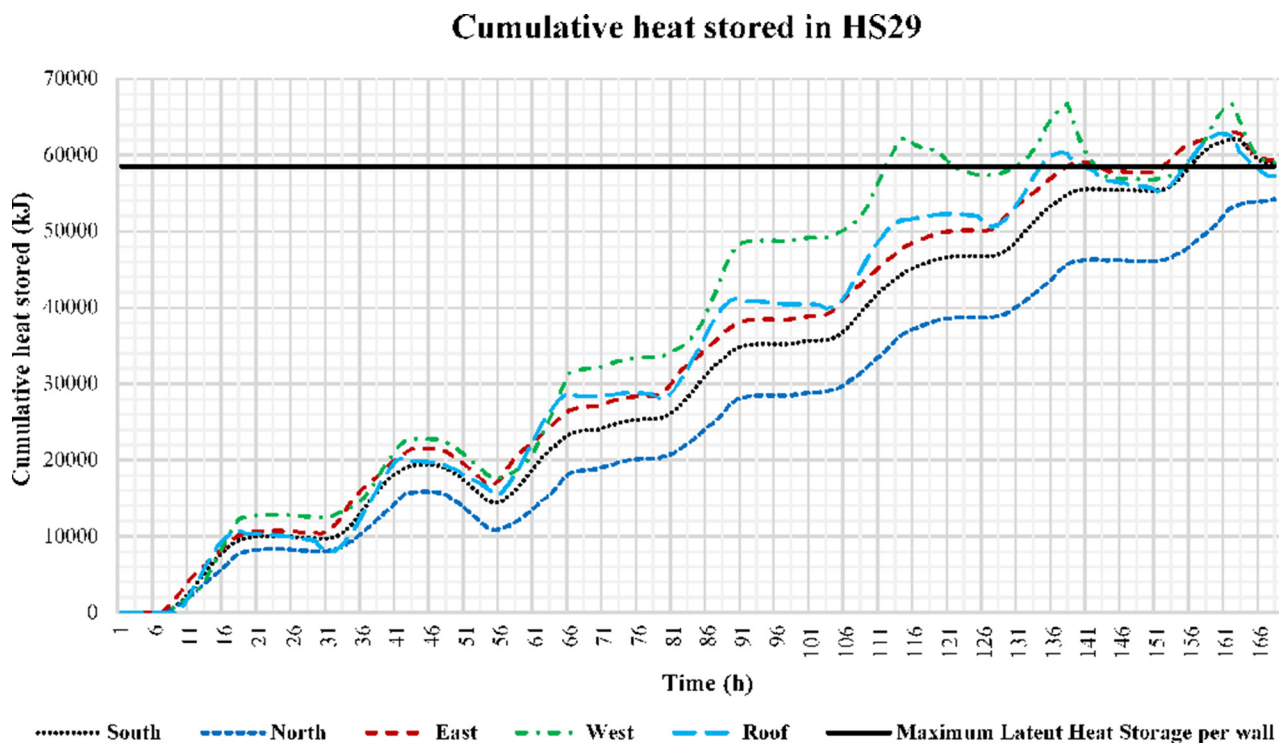


Fig. 15 Cumulative heat stored in HS29

four cases, viz., without any PCM and with HS29, OM32, and HS34. The heat flow is maximum in the case of wall without any PCM, followed by HS34, OM32, and HS29 incorporated wall, respectively. Similar observations are made from Figs. 10 to 13, showing the heat flow profile of west, east, and north facing walls and the roof, respectively, for all four cases, as mentioned earlier. The heat flow for without PCM case is higher due to two reasons: first is due to lower thermal resistance and second because of lower heat capacity of wall/roof. The PCM layer adds to both the thermal resistance as well as to the heat capacity of the composite wall. The latent heat absorbed can be more than 50 times the sensible heat that can be stored for per degree rise in temperature, thereby resulting in higher thermal mass of the building. Peaks are observed on the seventh day for the south wall (Fig. 9) and fifth

day onwards, for the west wall (Fig. 10), incorporated with HS29. This occurs due to complete melting of HS29 over the south and west walls, thus absorbing only the sensible heat and causing it to change its temperature rapidly resulting in a higher rate of heat transfer toward the conditioned space.

Figure 14 shows the comparison between the three PCMs, in terms of heat transfer to the conditioned space. It is observed that maximum amount of heat is transferred in case of HS34, followed by OM32, and then HS29. Comparing HS29 with OM32, the thermal conductivity is almost half, for OM32. Owing to the lower thermal conductivity, it offers a higher resistance to heat flow; however, the heat transferred is relatively higher. The reason behind is its melting point, which plays a pivotal role here. At melting point, material starts absorbing

Cumulative heat stored in OM32

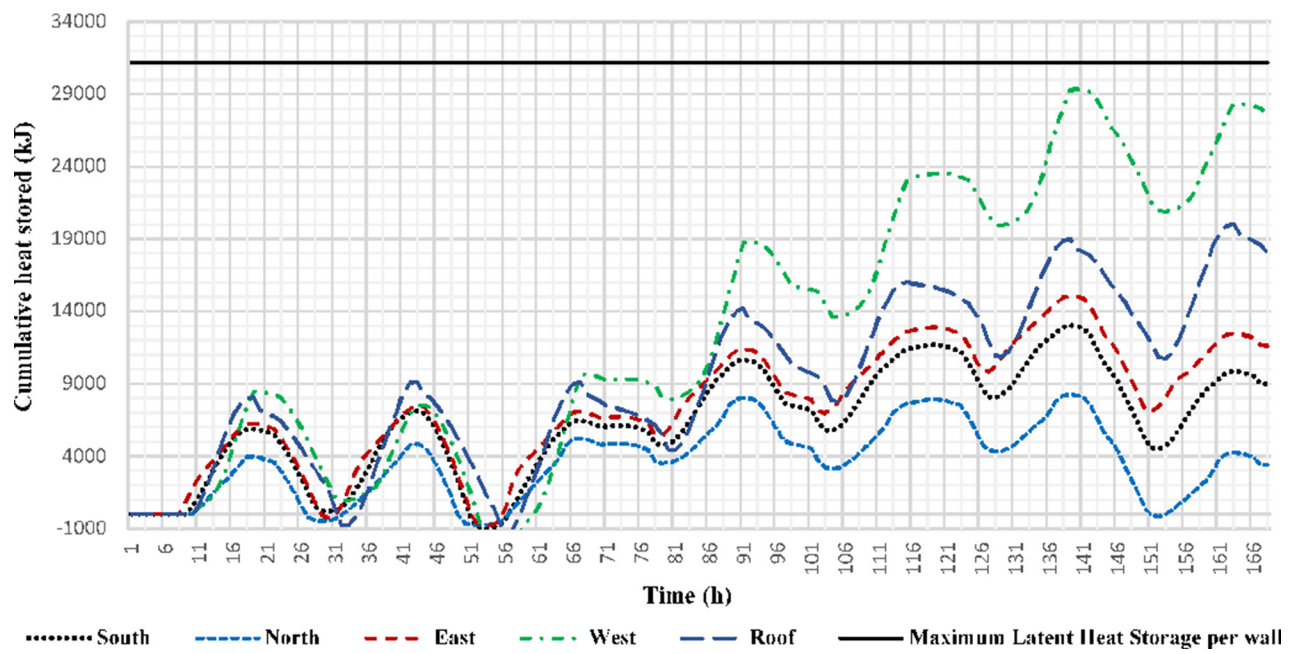


Fig. 16 Cumulative heat stored in OM32

latent heat, inhibiting the temperature change until the completion of the phase change process. Owing to the higher phase change temperature of OM32, the temperature difference between the PCM layer and conditioned space also increases, resulting in higher rate of heat flow to the conditioned space during phase change. Once the phase change is completed, sensible heating of PCM starts, thereby increasing the temperature

more rapidly. This explanation holds true for the higher heat flow in the case of HS34 as well. The graph clearly shows that heat flow rate is constant with respect to time when temperature of the PCM is equal to the phase change temperature. It is quite evident that this graph does not explain about the heat stored within the PCM that is to be calculated to account for the charging and discharging of the PCMs.

Cummulative heat stored in HS34

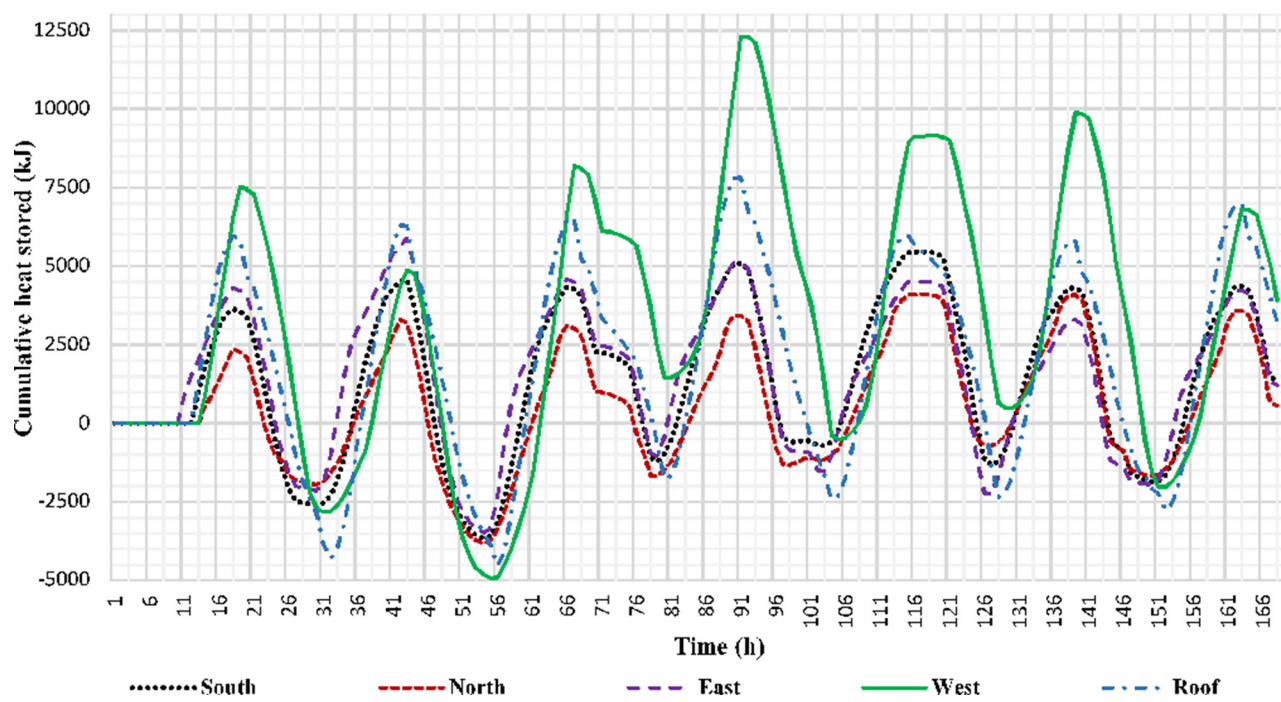


Fig. 17 Cumulative heat stored in HS34

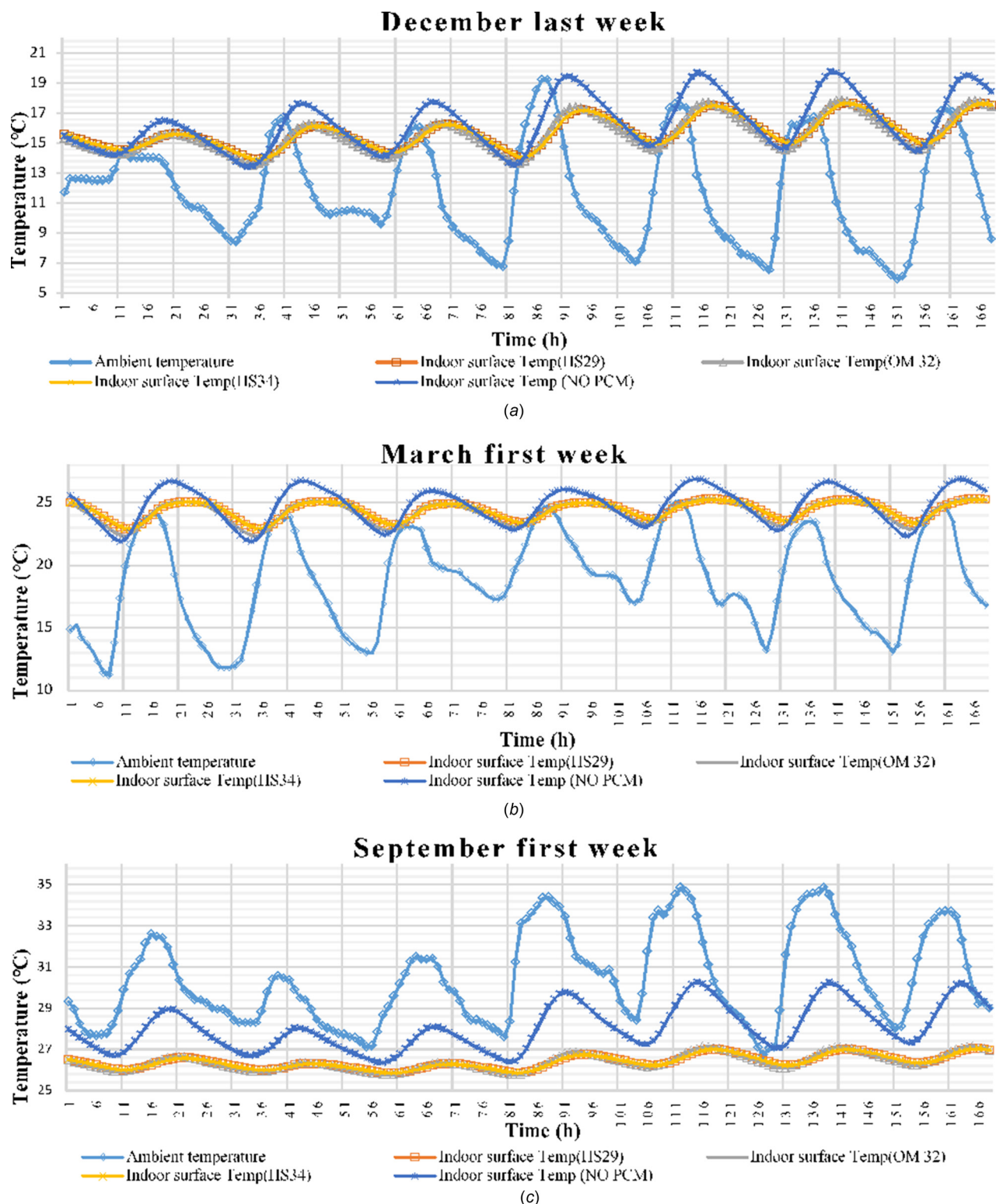


Fig. 18 (a) Inside temperature comparison for PCMs during last week of December. (b) Inside temperature comparison for PCMs during first week of March. (c) Inside temperature comparison for PCMs during first week of September.

Figures 15–17 show the cumulative heat stored within the three PCMs, calculated using the mathematical modeling. The bold line (in Figs. 15 and 16) shows the maximum amount of latent heat that can be stored within the PCM, which is equal to the product of their mass and corresponding latent heats. It is seen that in the case of HS29 (refer Fig. 15), the contours show a rising trend, which means there is an overall addition to the heat content of the PCM, day after day. This depicts the lack of discharging during

the night hours thereby, causing it to melt completely in almost all the cases/surfaces and making it unsuitable for the subsequent cycles. Similar explanation underlies for OM32. Due to lack of discharging due to insufficient temperature difference between its phase change temperature and the ambient temperature during off-sunshine hours would result in complete melting of the PCM soon. Thus, it is also regarded as unsuitable for summer conditions in New Delhi. The analytical results for HS34 (refer Fig. 17) show

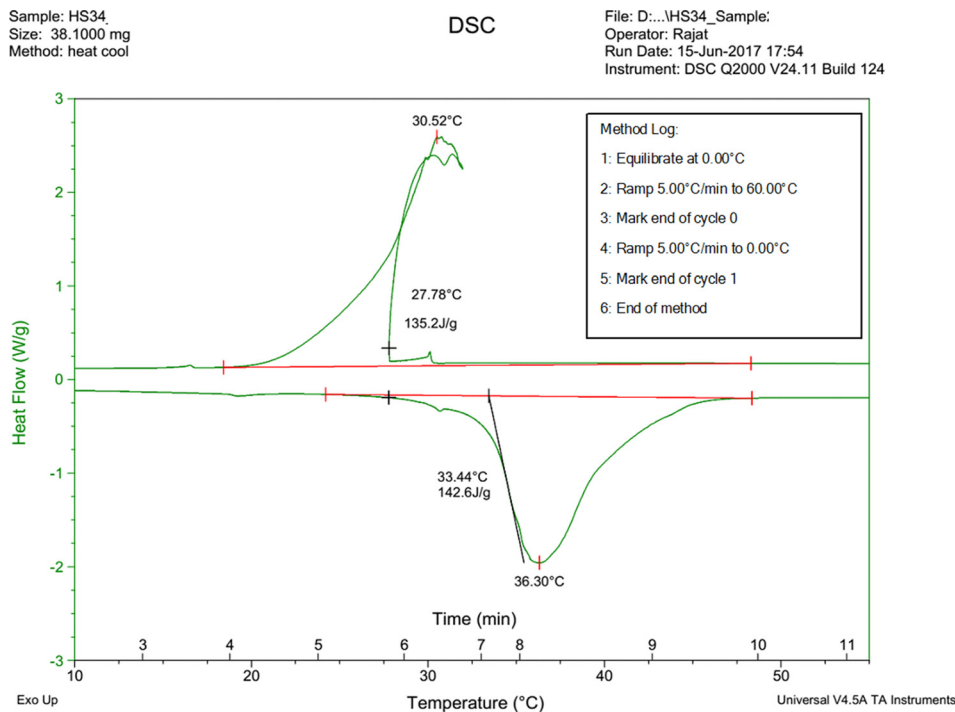


Fig. 19 Heating and cooling curve for HS34 from differential scanning calorimeter (DSC)

that it is discharged completely during the night hours and has a storage capacity left to support higher solar heat influx. The cumulative heat stored attains a negative value showing that it discharges completely during the night. It also indicates that the thickness of PCM can also be reduced, thereby resulting in reduction of PCM cost. The heat flow to the conditioned space, in the case of HS34, is much higher as compared to the other two PCMs, yet it is nearly half of the heat transferred for without PCM case. During off-sunshine hours, the PCM temperature is higher than both the conditioned space and the ambient. Thus, the heat flow takes place in both the directions, thereby reducing the overall heat flow to the conditioned space.

5.2 Assessment of PCMs Under Different Temperature Conditions. To access the effectiveness of PCMs under different temperature conditions an ENERGYPLUS simulation is carried out for three different weeks, other than summer season, to account for the temperature variation during the year. December end accounts for peak winters in Delhi, thus December last week is chosen for the study. March first week and September first week are chosen to account for their distinct temperature variation during the year. As the maximum heat influx is through the roof of any building, thus, Fig. 18 shows the comparison of inside surface temperature of the roof for different PCMs. Figure 18(a) shows that the lowest ambient temperature during December last week is 6 °C. The roof without PCM shows larger temperature variation as compared to the PCM incorporated roof. The mean temperature however is observed to be around 15.7 °C. The mean standard deviation between the different inside roof temperatures for PCMs was found to be equal to 0.16. Figure 18(b) shows the inside roof temperature for first week of March. The mean temperature during the period is equal to around 19 °C with a peak of 25.1 °C. The inside roof temperature in all the cases is around 24 °C; however, the temperature amplitude in case of PCM incorporated roof is relatively smaller. The mean standard deviation between the different inside roof temperatures for PCMs was found to be equal to 0.15. Figure 18(c) shows the inside roof temperature for first week of September. The mean ambient temperature during the period is

equal to around 30.4 °C with a peak of 35 °C. The inside roof temperature for the PCM incorporated roof is in around 26.4 °C. The mean standard deviation between the different inside roof temperatures for PCMs was found to be equal to 0.05. The comparison shows that the temperature variation in first week of September, first week of March and December last week, for the three PCMs is not considerable. However, it is also observed that amplitude of temperature variation for PCM incorporated roof is relatively small as compared to without PCM case. The results through ENERGYPLUS simulation show that temperature for the inside surface for all the PCMs is almost same; therefore, it can be concluded that the PCM impact is minimal when the ambient temperature is close to the phase change temperature. Thus, for all the temperature conditions except summer, all PCMs behave almost similarly resulting in almost same inside surface temperature and reduction in amplitude of temperature variation.

5.3 Characteristic Charging and Discharging of HS34. **DSC experiment and data analysis:** Based on the analytical results, HS34 is found to be most suitable. To ratify this, the heat flow analysis of HS34 on differential scanning calorimeter (DSC-Q2000, TA, Newcastle, DE) is carried out. The experimental temperature range is kept from 0 °C to 60 °C at a constant heating and cooling rate of 5.0 °C/min. The temperature accuracy and calorimetric precision are ± 0.01 °C and $\pm 0.05\%$, respectively. HS34 is first melted and stirred using an electromagnetic stirrer/hot plate. The sample is then placed in an aluminum sample pan (Tzero pan, no: 160217, Swiss make) with a lid (Tzero lid, no: T160316, Swiss make), and the DSC experiment is conducted under high-purity nitrogen at a flow rate of 50 ml/min. The experiment is carried out on a sample mass of 38.1 mg measured using a precision electronic balance (GR-202, A&D, Tokyo, Japan) with a precision of 0.1 mg. The DSC results are analyzed by a computer software (Universal Analysis 2000, TA) for temperature range of 10 °C to 55 °C to assess the heat flow curve and phase change temperature range for both heating and cooling of the PCM.

Figure 19 shows heating and cooling curve of HS34. It shows incongruent behavior while melting and solidification. During

melting, the melting onset temperature and peak melting temperature is equal to 33.44°C and 36.30°C, respectively. During solidification, the peak solidification temperature is observed to be 30.52°C, which is around 6°C below its peak melting temperature. This is due to the super-cooling effect shown by the hydrated salts. It is observed that solidification process is completed close to 24°C. The ripples formed during solidification depicts the difference in the solidus temperature of constituent salts, thus, showing it to be a heterogeneous mixture. The super-cooling shown by HS34 makes it unsuitable for peak summer conditions of New Delhi as it may not solidify during the night hours due to its lower phase change temperature.

6 Conclusions

This study provides the quantitative comparison of three PCMs HS29, OM32, and HS34 for composite climate. Following inferences are drawn by carrying out this study:

- (1) The PCM incorporation in buildings has high energy saving potentials; however, for efficient utilization of PCM, there is a need, to map them to the particular climatic condition.
- (2) The effective heat flow to the conditioned space is reduced with PCM incorporation. This is because only a part of heat stored within the PCM during the day flows to the conditioned space and rest flows to the ambient, during the off-sunshine hours. It is also observed that PCM incorporation reduces the amplitude of temperature fluctuations within a building space.
- (3) The study postulates that suitability of any PCM should be gauged based on the cumulative heat stored within the PCM, instead of heat transferred to the conditioned space. The heat flow in the case of HS29 and OM32 is less by 55% and 22%, respectively, than in the case of HS34. However, it is seen that the cumulative heat stored in the PCM gives a clearer picture about the suitability of PCM, as it shows whether PCM discharges completely during the off-sunshine hours or not.
- (4) It is necessary for the PCMs to discharge/recharge during the off-sunshine hours, to be available for energy storage on the subsequent day. Mathematical modeling showed that phase change temperature of 34°C is suitable for New Delhi, thus, only HS34 designated as suitable; however, the heat flow analysis through DSC showed that it is a heterogeneous mixture of salts showing super-cooling of around 6°C making it unsuitable for peak summers in New Delhi.

Acknowledgment

Authors are thankful to Professor S. C. Kaushik for his indelible help, support, and guidance. We would like to acknowledge Ministry of Human Resource & Development and Department of Science & Technology, Government of India, for the financial support. We are also thankful to PLUSS Advanced Technologies Pvt. Ltd., for providing the samples for this study.

Nomenclature

c_p	= specific heat at constant pressure (J/kg·K)	γ	= solar azimuth angle
h_i, h_o	= internal and ambient convective heat transfer coefficients (W/m ² ·K)	θ_i	= angle of incidence
I, I_d, I_b	= horizontal global, diffuse and beam irradiance (W/m ²)	θ_z	= solar zenith angle
I_o	= extra-terrestrial irradiation (W/m ²)	ρ	= density (kg/m ³)
k_1, k_2, \dots, k_n	= thermal conductivities (W/m·K)	ϕ	= latitude
L_{st}, L_{loc}	= longitude standard and local	ω	= solar hour angle
T_{sol}	= solar air temperature (K)		
t_o, t_i, t_{wall}	= ambient, room and wall temperatures		
U	= universal heat transfer coefficient (W/m ² ·K)		
β	= tilt of the surface		

- [24] Diaconu, B., and Cruceru, M., 2010, "Phase Change Material (PCM) Composite Insulating Panel With High Thermal Efficiency," International Conference on Recent Advances in Energy and Environment Technologies and Equipment (EEETE), Bucharest, Romania, Apr. 20–22, pp. 105–110.
- [25] Arora, C. P., 2009, *Refrigeration and Air Conditioning*, Tata McGraw-Hill Education, New Delhi, India.
- [26] Tiwari, S., Tiwari, G. N., and Al-Helal, I. M., 2016, "Performance Analysis of Photovoltaic-Thermal (PVT) Mixed Mode Greenhouse Solar Dryer," *Sol. Energy*, **133**, pp. 421–428.
- [27] Tabares-Velasco, P. C., Christensen, C., Bianchi, M., and Booten, C., 2012, "Verification and Validation of EnergyPlus Conduction Finite Difference and Phase Change Material Models for Opaque Wall Assemblies," National Renewable Energy Laboratory, Golden, CO, Report No. [NREL/TP-5500-55792](#).
- [28] Pedersen, C. O., 2007, "Advanced Zone Simulation in EnergyPlus: Incorporation of Variable Properties and Phase Change Material (PCM) Capability," Building Simulation Conference, Beijing, China, Sept. 3–6, pp. 1341–1345.